Supplementary Information

Light-induced electron transfer/phase migration of a redox mediator for photocatalytic C–C coupling in a biphasic solution

Ren Itagaki,[a] Shin-ya Takizawa,[b] Ho-Chol Chang,[a] and Akinobu Nakada[a,c]**

[a]Department of Applied Chemistry, Faculty of Science and Engineering, Chuo University, 1-13-27 Kasuga, Bunkyo-ku, Tokyo 112-8551, Japan

[b]Department of Basic Science, Graduate School of Arts and Sciences, The University of Tokyo, 3-8-1 Komaba, Meguro-ku, Tokyo 153-8902, Japan

[c]Precursory Research for Embryonic Science and Technology (PRESTO), Japan Science and Technology Agency (JST), 4-1-8 Honcho, Kawaguchi, Saitama 332-0012, Japan

*E-mail: chang@kc.chuo-u.ac.jp (H.C.), nakada@scl.kyoto-u.ac.jp (A.N.)

Table of Contents

p.3 **Fig. S1** Cyclic voltammogram of Bn-Br in DCE

p.4 **Fig. S2** Emission spectra of **Ru** or **Ir** with Bn-Br in DCE

p.5 **Fig. S3** UV-vis absorption and emission spectra of Fc and Bn-Br, in DCE

p.6 **Fig. S4** Emission decays of **Ru** and **Ir** in DCE

p.7 **Fig. S5** HPLC chromatograms before and after photocatalysis

p.8 **Fig. S6** UV-vis absorption spectra of $Fc^+PF_6^-$ and Fc^+Cl^- in an aqueous phase

p.9 **Table S1** Photocatalytic activity of Bn-Br reduction in DCE solution

p.11 **Fig. S7** ^{1}H NMR spectra of **Ru** and **Ir**

p.12 **Fig. S8** EDX spectra of $Fc^+PF_6^-$ before and after Cl^- ion exchange

p.13 **Fig. S9** Photographs of H_2O/DCE (1:1) biphasic reaction solution

p.14 **Fig. S10** HPLC chromatograms of Bn-Br, Fc, and Bn_2

p.15 **References**

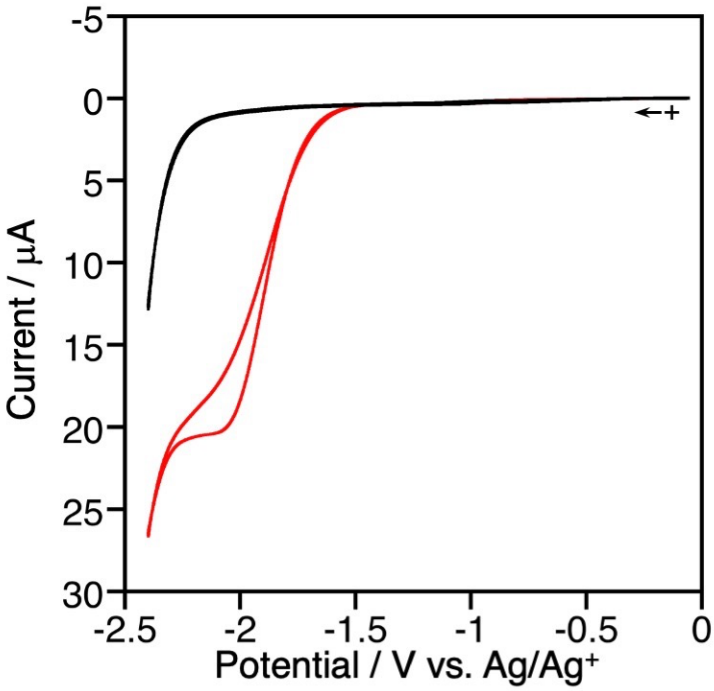

Fig. S1 Cyclic voltammograms of Bn-Br (red; 1 mM) and blank (black) in DCE containing NBu_4PF_6 (0.1 M) as the supporting electrolyte; scan rate: 0.005 V s^{-1}; working electrode: glassy carbon; reference electrode: $Ag/AgNO_3$ (0.01 M); counter electrode: Pt wire.

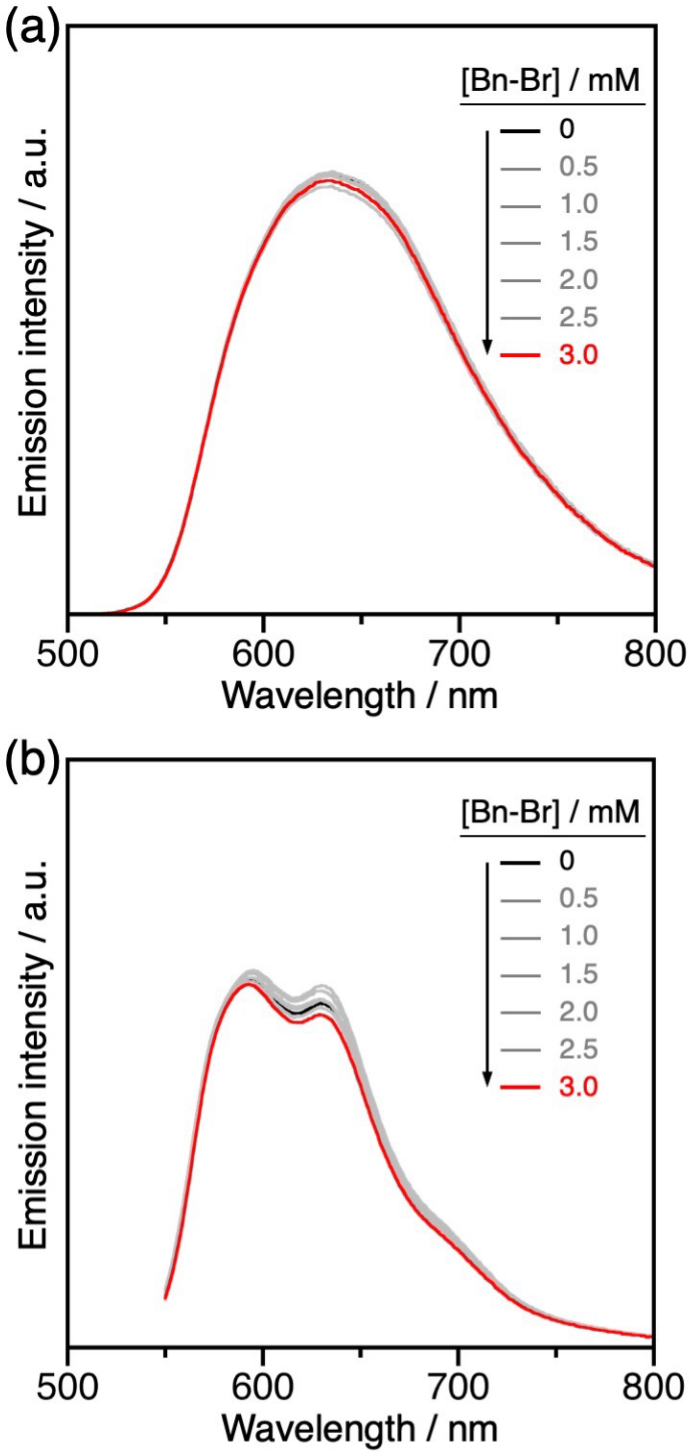

Fig. S2 (a) Emission spectra of **Ru** (b) and **Ir** (c) in the presence of Bn-Br (0–3.0 mM) in DCE. The excitation wavelengths were 460 nm and 480 nm for **Ru** and **Ir**, respectively.

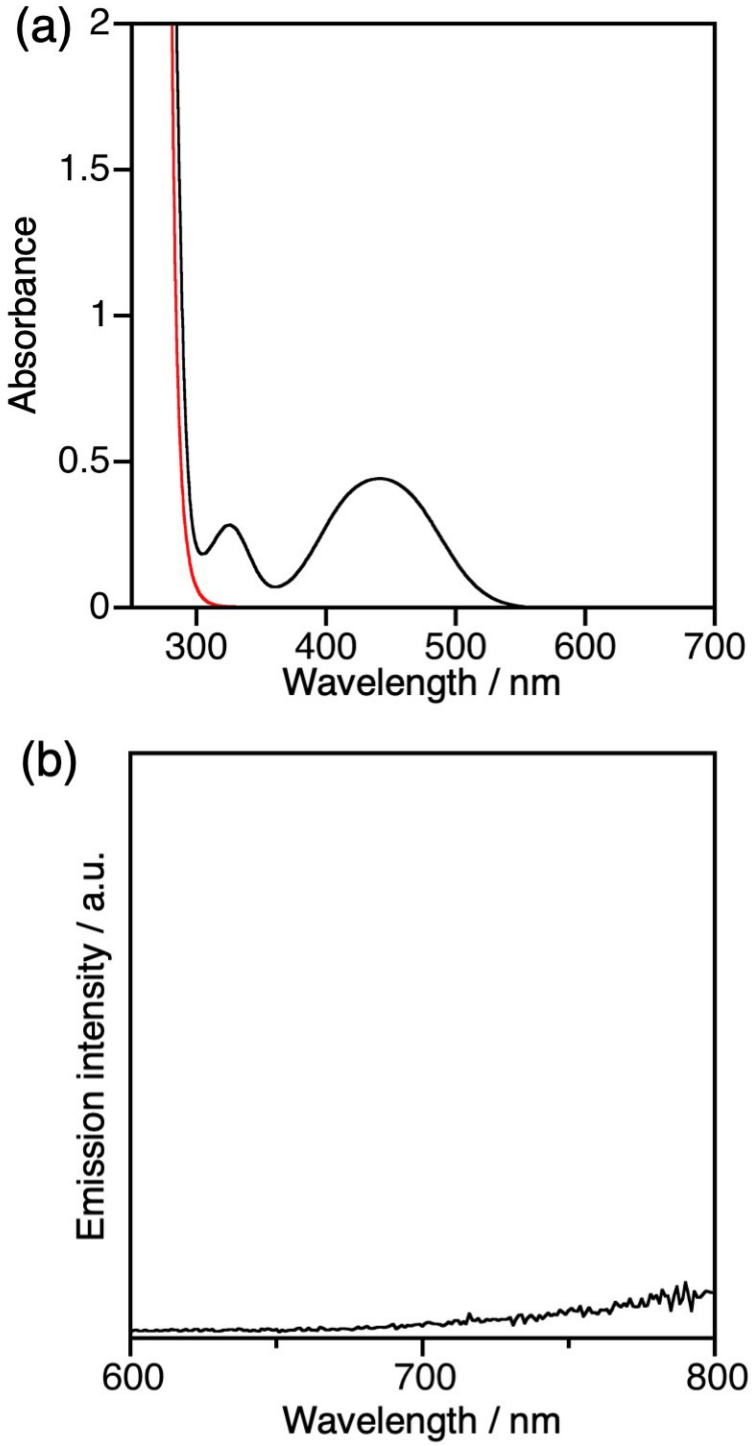

Fig. S3 (a) UV-vis absorption spectra of Fc (5 mM, black) and Bn-Br (50 mM, red), as well as (b) emission spectrum of Fc (λ_{ex} = 460 nm) in DCE.

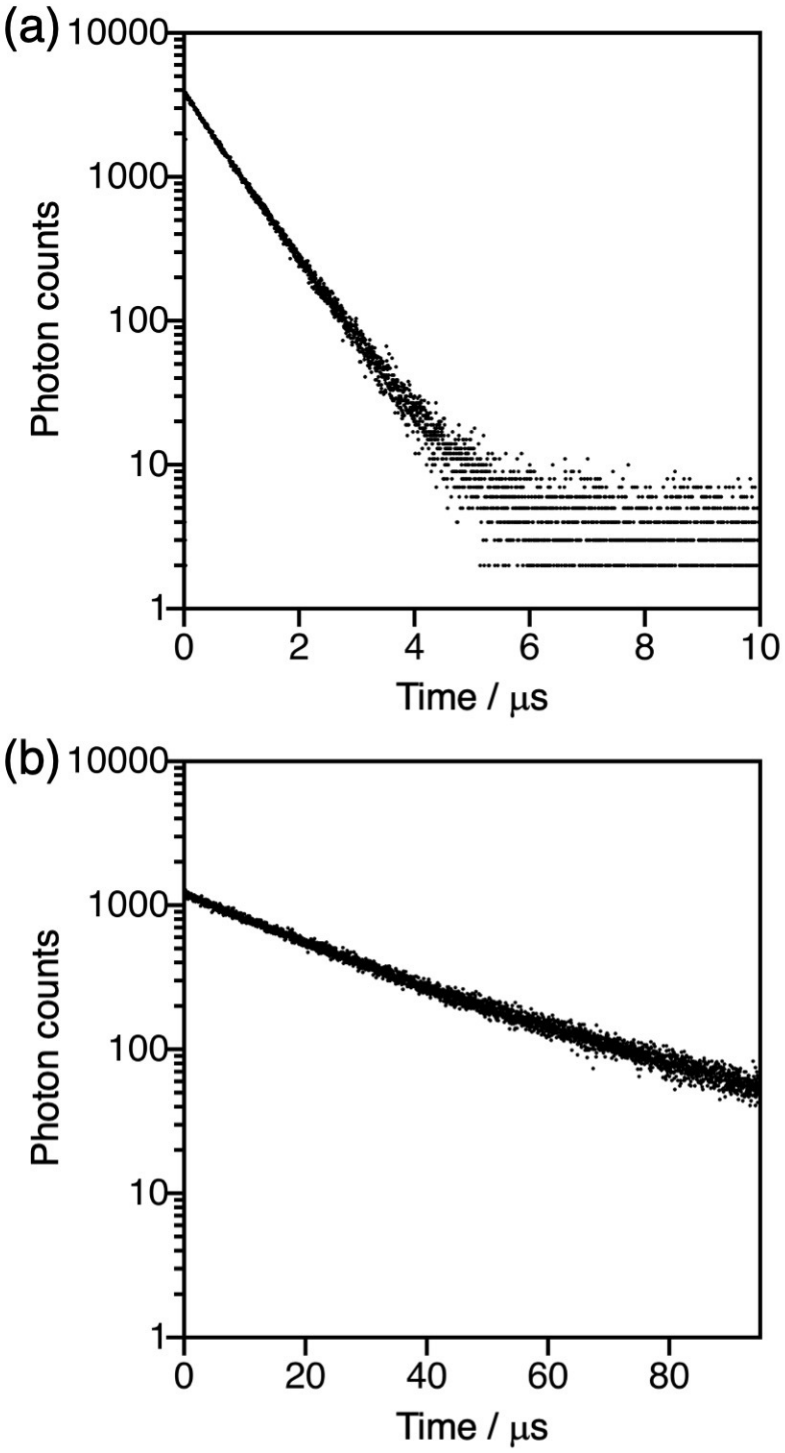

Fig. S4 Emission decay (a) at 620 nm from **Ru** (0.006 mM) and (b) at 590 nm from **Ir** (0.00025 mM) in DCE (λ_{ex} = 440 nm).

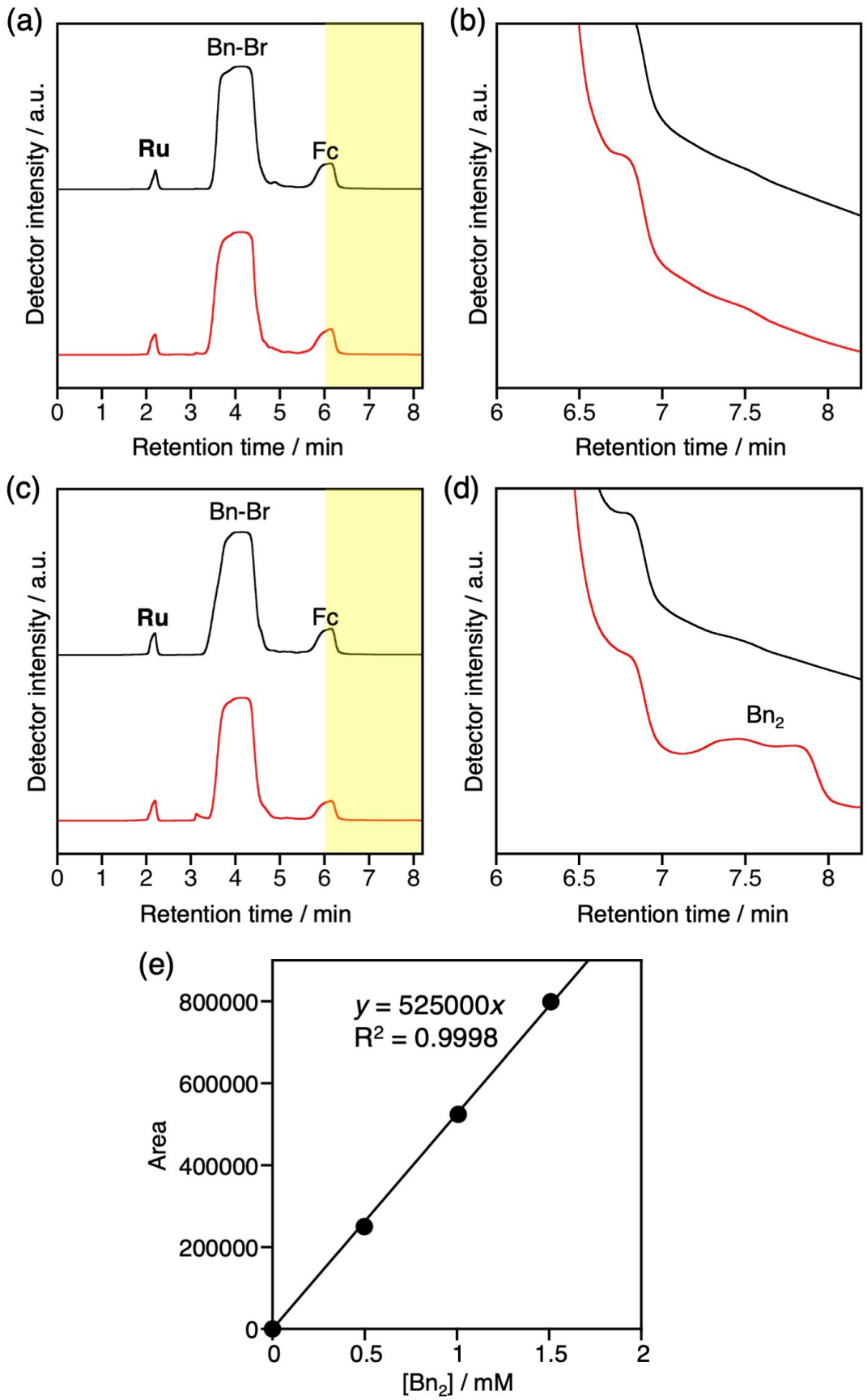

Fig. S5 HPLC chromatograms of DCE containing **Ru** (0.5 mM), Fc (5 mM), and Bn-Br (50 mM) (a,b) in the absence and (c,d) presence of aqueous phase before (black) and after (red) irradiation with visible light (λ > 400 nm) for 1 h; (b,d) show a magnification of the yellow highlighted area in (a,c), which corresponds to the peak for Bn_2. (e) Calibration curves of Bn_2 based on HPLC areas. For further characterization of each peak, see Fig. S10.

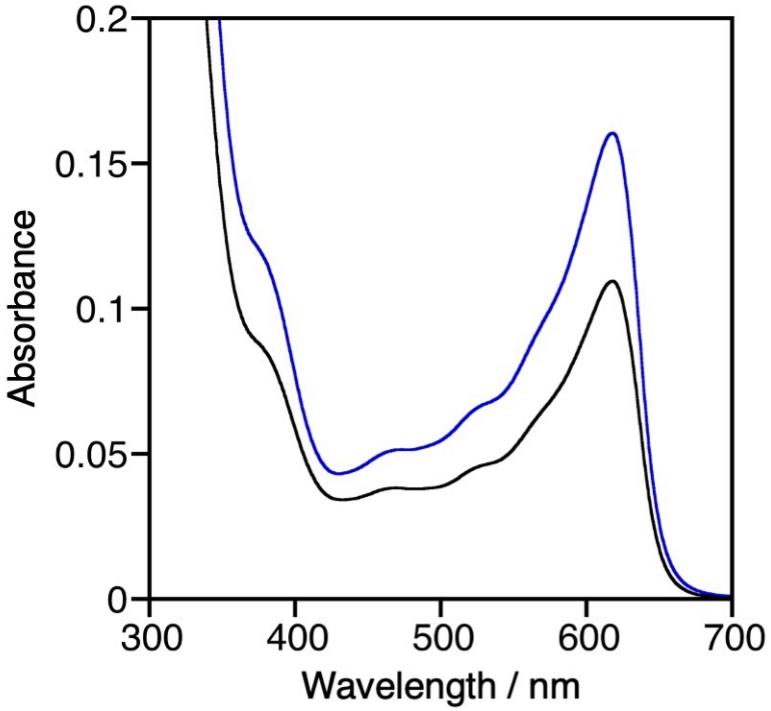

Fig. S6 UV-vis absorption spectra of the aqueous phase of a H_2O/DCE biphasic solution containing 7.5 μmol of $Fc^+PF_6^-$ (black) and Fc^+Cl^- (blue) measured after stirring for 10 min under a nitrogen atmosphere.

Table S1 Photocatalytic activity of the Bn-Br reduction using various photosensitizers and sacrificial electron donors in single-phase organic solution.

Entry	Photosensitizer	Sacrificial electron donor	Solvent	TOF/ h^{-1} (TON)	Quantum yield	Ref.
1	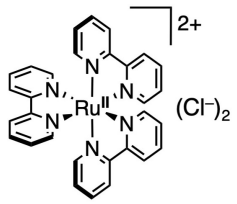	BNAH[a]	MeCN	65.7 (164.3)	0.65[b]	S1
2	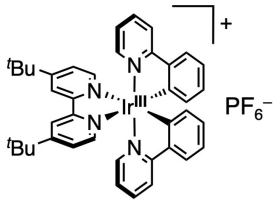	Hantzsch ester	DMF	24.0 (96.0)	–	S2
3[c]	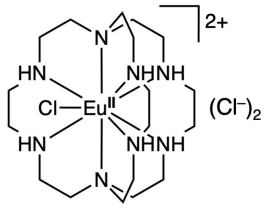	Zinc dust	MeOH	20.0 (120.0)	–	S3
4	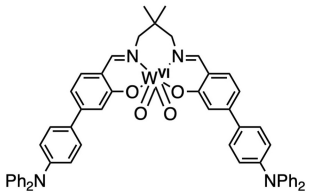	B_2Pin_2[d]	MeCN	7.9 (94.8)	–	S4
5[c]	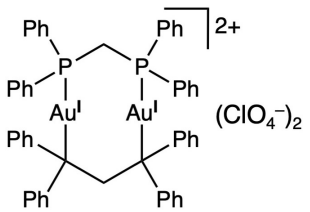	NEt_3	MeCN	7.2 (172)	–	S5
6	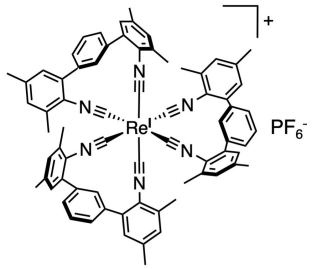	DIPEA[e]	CD_2Cl_2	4.1 (81.0)	–	S6
7	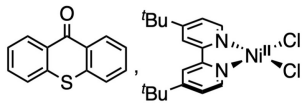	NEt^iPr_2	^{t}BuOH	1.4 (16.8)	–	S7
8	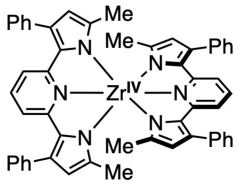	^{MeO}BIH[f]	C_6D_6	1.1 (12.8)	0.0039	S8

Entry	Photosensitizer	Sacrificial electron donor	Solvent	TOF/ h^{-1} (TON)	Quantum yield	Ref.
9[c]	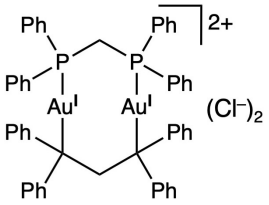	NEt_3	CD_3OD/ CD_3CN (1:1)	1.0 (4.8)	–	S9
10	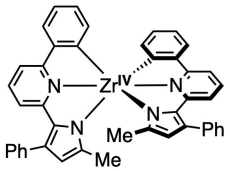	BIH[g]	C_6D_6	1.0 (2.0)	–	S10
11[c]	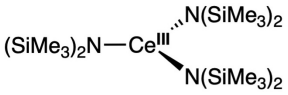	$NaN(SiMe_3)_2$	Et_2O	0.4 (19.0)	–	S11

[a]1-benzyl-1,4-dihydronicotinamide. [b]Quantum efficiency for BNAH consumption; that of Bn_2 was not reported. [c]Photoreduction of benzyl chloride. [d]Bis(pinacolato)-diboron. [e]*N*,*N*-diisopropylethyamine. [f]1,3-dimethyl-2-phenyl-2,3-dihydro-1*H*-7-methoxybenzo[*d*]imidazole. [g]1,3-dimethyl-2-phenyl-2,3-dihydro-1*H*-benzo[*d*]imidazole.

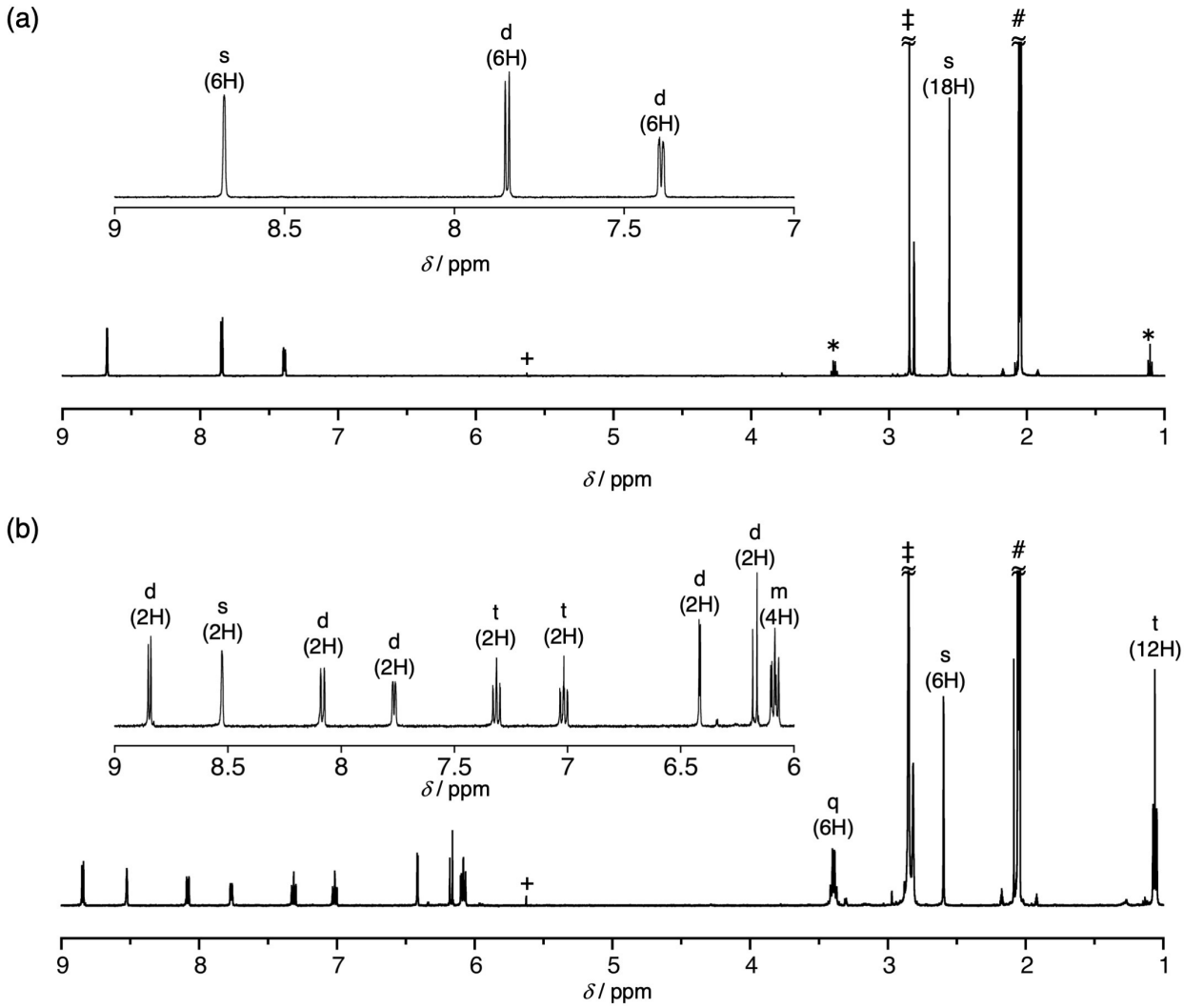

Fig. S7 ^{1}H NMR spectra of (a) **Ru** and (b) **Ir** (500 MHz, acetone-d_6). The symbols "‡", "#", "*", and "+" indicate signals that arise from residual protons of H_2O, acetone, Et_2O, and CH_2Cl_2, respectively; insets: enlarged aromatic region of the ^{1}H NMR spectra.

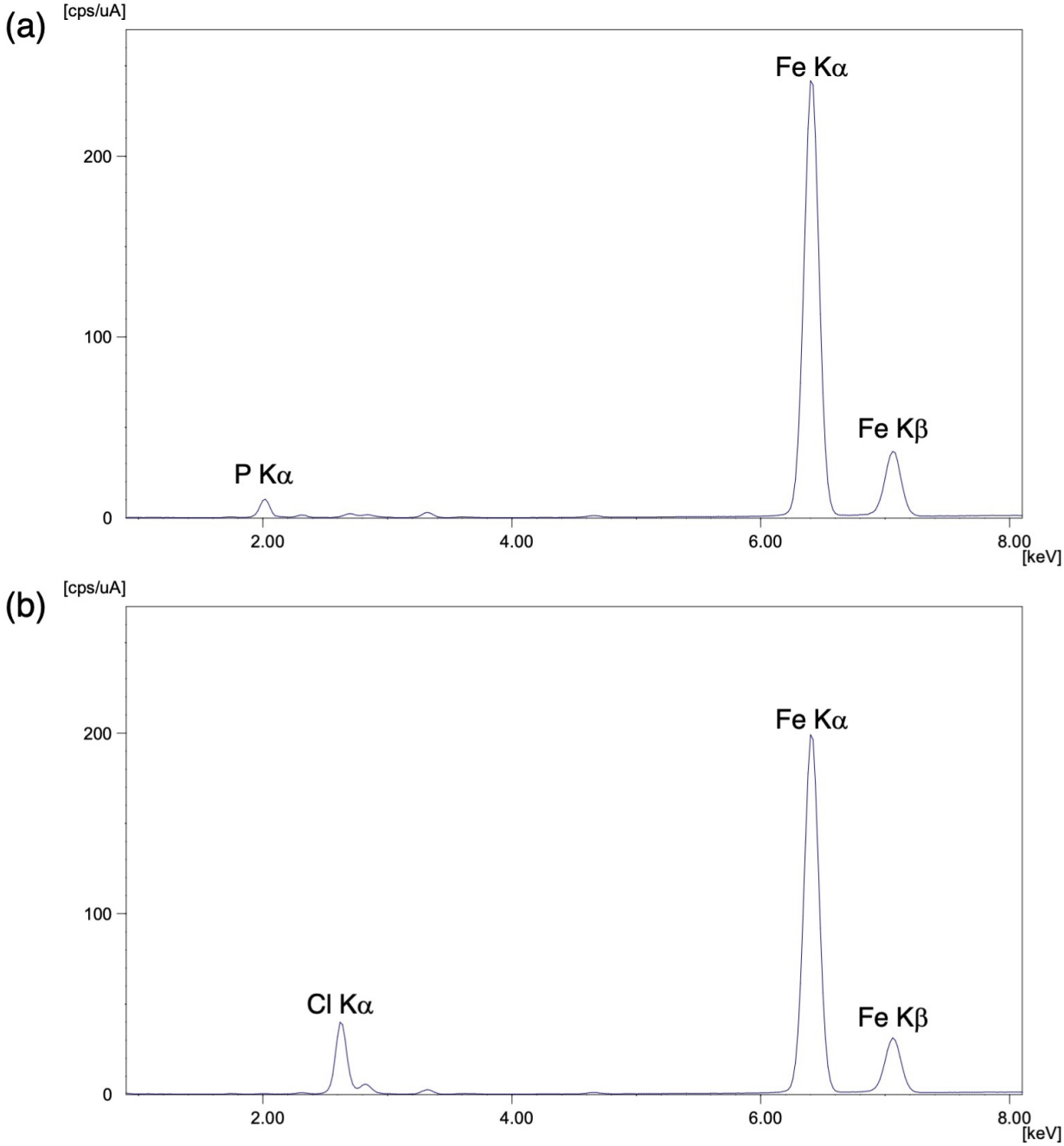

Fig. S8 Electron dispersion X-ray spectra of $Fc^{+}PF_6^{-}$ (a) before and (b) after treatment with the Cl^{-} ion-exchange resin.

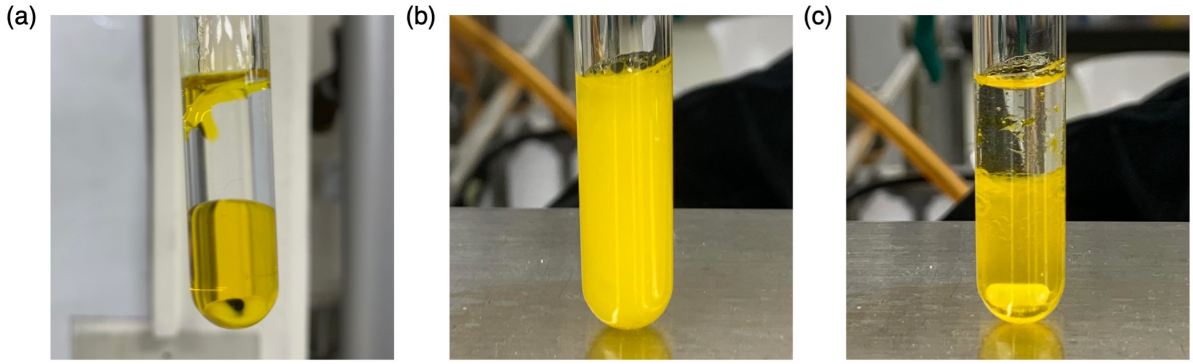

Fig. S9 Photographs of a H_2O/DCE (1:1, *v*/*v*) biphasic solution containing **Ir** (0.5 mM), Fc (5.0 mM), and Bn-Br (50 mM) (a) before, (b) during, and (c) after stirring.

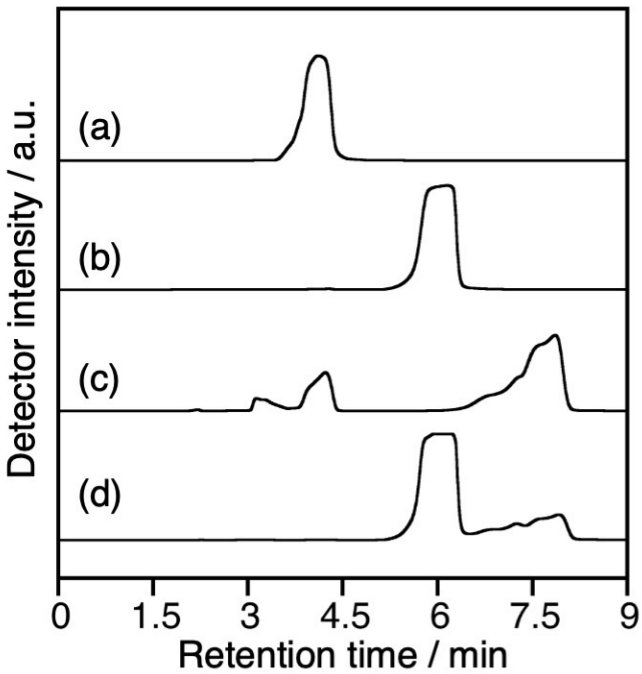

Fig. S10 HPLC chromatograms of DCE solutions containing (a) Bn-Br, (b) Fc, (c) Bn_2, and (d) a mixture of Fc and Bn_2.

References

S1. K. Hironaka, S. Fukuzumi and T. Tanaka, *J. Chem. Soc. Perkin Trans. 2*, 1984, 1705-1709.

S2. G. Park, S. Y. Yi, J. Jung, E. J. Cho and Y. You, *Chemistry*, 2016, **22**, 17790-17799.

S3. T. C. Jenks, M. D. Bailey, J. L. Hovey, S. Fernando, G. Basnayake, M. E. Cross, W. Li and M. J. Allen, *Chem. Sci.*, 2018, **9**, 1273-1278.

S4. D. Yu, W. P. To, G. S. M. Tong, L. L. Wu, K. T. Chan, L. Du, D. L. Phillips, Y. Liu and C. M. Che, *Chem. Sci.*, 2020, **11**, 6370-6382.

S5. D. Li, C.-M. Che, H.-L. Kwong and V. W.-W. Yam, *J. Chem. Soc., Dalton Trans.*, 1992, 3325-3329.

S6. C. B. Larsen and O. S. Wenger, *Inorg. Chem.*, 2018, **57**, 2965-2968.

S7. Y. Masuda, N. Ishida and M. Murakami, *Eur. J. Org. Chem.*, 2016, **2016**, 5822-5825.

S8. Y. Zhang, T. S. Lee, J. L. Petersen and C. Milsmann, *J. Am. Chem. Soc.*, 2018, **140**, 5934-5947.

S9. H. Tran, T. McCallum, M. Morin and L. Barriault, *Org. Lett.*, 2016, **18**, 4308-4311.

S10. Y. Zhang, J. L. Petersen and C. Milsmann, *Organometallics*, 2018, **37**, 4488-4499.

S11. H. Yin, P. J. Carroll, J. M. Anna and E. J. Schelter, *J. Am. Chem. Soc.*, 2015, **137**, 9234-9237.